ULTRAVIOLET PROPERTIES OF CRYSTALLINE ANTHRACENE

W. H. WRIGHT

Southwest Center for Advanced Studies, Dallas, Texas

Received March 30, 1967

CONTENTS

I. INTRODUCTION

Anthracene has been subjected to a good deal of experimental and theoretical investigation both for practical purposes (it is carcinogenic and a good scintillator) and for academic reasons, it being a relatively simple representative of a large and interesting class of substances. This review deals principally with experiments performed on single crystals with ultraviolet radiation; absorption, reflection, photoconduction, and fluorescence are the major areas reviewed. In order to interpret the experiments it is necessary to have some knowledge of the theoretical work on the energy levels in the crystal, and the earlier sections of this article are devoted to a brief outline of this theory.

No complete review of these ultraviolet properties appears to have been written, although some of them have been briefly described in review articles covering different fields, *e.g.*, triplet excitons (71) and electron energy transfer between organic molecules (118). This review covers systematically the work reported to the end of 1965 and includes some references later than this date where the papers have been easily available.

II. STRUCTURE OF THE MOLECULE AND CRYSTAL

Anthracene ($C_{14}H_{10}$) is an aromatic organic compound, the molecule consisting of three benzene rings. Two of these molecules fit into a unit cell as shown in

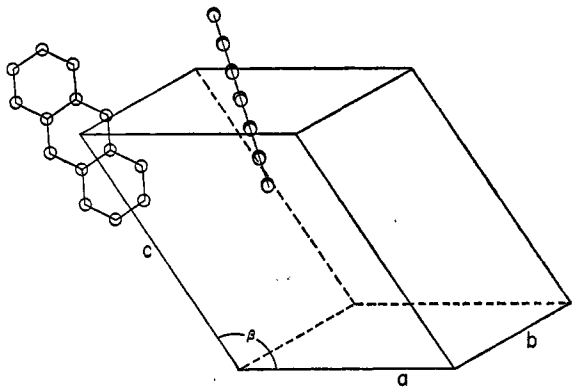

Figure 1.—Anthracene molecules in a unit cell.

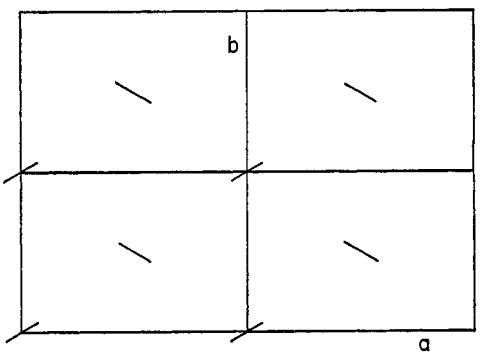

Figure 2.—Disposition of anthracene molecules in the (*ab*) crystal face.

Figure 1, one at a corner and the other at the center of the *ab* face of the unit cell. One can be transformed into the other by reflection in the *ac* plane and translation along the *a* axis by *a*/2. The unit cell has dimensions $a = 8.561$ A, $b = 6.036$ A, $c = 11.163$ A, and the angle β is 124° 24′.

The anthracene crystal belongs to the monoclinic normal class; *i.e.*, it has one twofold axis of symmetry (the *b* axis) and a center of symmetry. Almost all experiments performed on anthracene have used the (001) crystal face, a face along which perfect cleavage is possible, and which contains the *a* and *b* axes. The molecules are seen end on from this face as shown in Figure 2. Full details of the crystallographic structure can be obtained (79, 110).

Quick identification of the planes and axes of anthracene can be achieved by the following method (85), if the accuracy obtainable from polarizing microscopes is not required. First the (001) face can be found because of its perfect cleavage, which reveals a smooth, shiny surface. The crystal is then cut in the form of a plate with the (001) faces in the plane of the plate. This plate is placed on a sheet of paper with a thin, straight line drawn on it. In general, double refraction causes two images of the line to be seen through the plate. As the plate is rotated about a normal axis, the double refraction disappears at two positions 180° apart, where the *a* axis lies along the line. Therefore the *b* axis, which lies in the plane of the plate, is at right angles to the line drawn on the paper. The remaining axes and major faces can be identified from the geometry described in the beginning of this section.

III. Molecular Energy Levels

A. π-Molecular Orbitals in Benzene

Molecular orbital methods have proved better than the valence bond approach in calculating the energy levels of the anthracene molecule. The valence bond method (70) has led to erroneous conclusions as to the nature and number of the excited states and will not be considered here.

It is convenient to start the treatment of the anthracene molecular energy levels with the consideration of benzene, since anthracene consists of three benzene rings. Trigonal hybridization occurs in the carbon atoms of benzene: a hybrid is formed between the 2s, $2p_x$, and $2p_y$ orbitals giving three directed new bonds in the *xy* plane which are mutually inclined at 120°. Thus the six carbon atoms in benzene lie in a plane, forming a regular hexagon; the six hydrogen atoms also lie in this plane. Each of the six carbon atoms is joined by σ orbitals to one hydrogen atom and to the adjacent two carbon atoms. The six $2p_z$ electrons are distributed among a set of molecular orbitals formed by linear combination of these atomic $2p_z$ orbitals, resulting in π bonds.

The $2p_z$ orbitals are delocalized since the wave functions describing each of them, ψ_n ($n = 1, 2, \ldots, 6$), overlap their two neighbors equally. Therefore the molecular orbitals are given by the linear combination

$$\psi = C_1\psi_1 + C_2\psi_2 + \ldots + C_6\psi_6 \qquad \text{(Eq 1)}$$

with the constants $C_1, C_2, \ldots, C_6$ determined by the fact that they should lead to stationary states. Equation 1 defines the π-type molecular orbitals of benzene. There are six independent combinations of this equation yielding six π-molecular orbitals each with a definite energy. The six π electrons are distributed among these orbitals, yielding for each distribution a π-electron configuration. The configuration for the ground state will obviously have two electrons in each of the three lowest orbitals. The other configurations provide a wide variety of excited states. The electronic transitions between such configurations were named N → V transitions by Mulliken (84). The characteristic spectral properties of benzene (and anthracene) are almost entirely due to these N → V transitions. Therefore, in the investigation of the absorption spectrum of the molecule, all except the π electrons can be ignored. There are several such theoretical treatments in existence, and the main points of some of these, as applied to anthracene, are considered in the following sections.

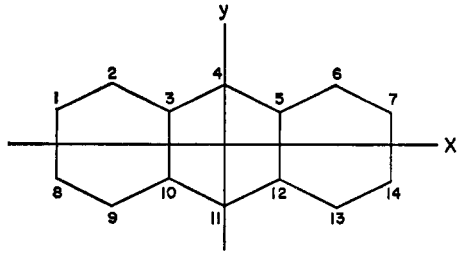

Figure 3.—The anthracene molecule.

B. COULSON'S LCAO APPROACH

The anthracene molecule, shown in Figure 3, has three twofold rotation axes of symmetry: the x, y, and z axes, as well as a plane of symmetry xy so that the full symmetry is D_{2h}. Detailed discussions of symmetry applied to this sort of problem are given by Mulliken (84) and Hochstrasser (53). One way of characterizing the symmetry properties of the allowed molecular orbitals is to label them in terms of what happens on reflection in the three fundamental planes. Using Coulson's notation (33–35) each orbital can be either symmetrical (S) or antisymmetrical (A). Since we are dealing with π orbitals, each of these molecular orbitals will be antisymmetric in the plane of the molecule and will therefore have the label A_z. Because this label is common to all these orbitals, it is often omitted from the descriptive symbol for the orbital, which would then be a combination of the remaining labels S_x or A_x, S_y or A_y.

The LCAO molecular orbitals of anthracene are given by

$$\psi = \sum_{1}^{14} C_r \psi_r \qquad \text{(Eq 2)}$$

The symmetry properties discussed above must be reflected in the values of the expansion coefficients C_r of Eq 2. Coulson indicates symmetry S_xS_y by P, A_xS_y by Q, S_xA_y by R, and A_xA_y by S.

The results of group theory show that for the D_{2h} symmetry there are only eight distinct types of molecular orbital, *viz.*, A_{1g}, A_{1u}, B_{1g}, B_{1u}, B_{2g}, B_{2u}, B_{3g}, and B_{3u}. Elementary arguments can be used to show that the types P, Q, R, and S correspond to the group theory symbols B_{1u}, B_{2g}, B_{3g}, and A_{1u}, respectively. The remaining four group theory symbols correspond to symmetry assignments similar to P, Q, R, and S but which have the common symmetry S_z instead of A_z. These are σ orbitals.

A detailed examination of Eq 2 shows that there are four molecular orbitals of each of the types P and R, and three each of Q and S. The relative energies of these 14 molecular orbitals have been calculated by Coulson (33, 35). The ground state is

$$P_1^2, Q_1^2, R_1^2, P_2^2, Q_2^2, S_1^2, R_2^2$$

where the suffixes have been assigned so that P_1 is lower than P_2, etc. Examination of Table I shows that two electrons sharing any one molecular orbital have combined symmetry A_{1g} and this, therefore, is the symmetry of the ground state. Table I shows the symmetry representation corresponding to any two electrons in any pair of orbitals of the types P, Q, R, and S.

TABLE I
SYMMETRY CLASS OF PRODUCT OF TWO ELECTRONS

	P	Q	R	S
P	A_{1g}	B_{3u}	B_{2u}	B_{1g}
Q	B_{3u}	A_{1g}	B_{1g}	B_{2u}
R	B_{2u}	B_{1g}	A_{1g}	B_{3u}
S	B_{1g}	B_{2u}	B_{3u}	A_{1g}

Each of the types of level could be either singlet or triplet while the ground state, with all orbitals doubly occupied, must be the singlet $^1A_{1g}$. Table I also indicates that for the g → u selection rule to hold, the only allowed transitions are to B_{2u} and B_{3u} configurations. The three allowed transitions of lowest energy obtained from Coulson's calculations of the relative energies of the 14 molecular orbitals are shown in Table II. Transition N → V_3 is forbidden because the excited configuration is B_{1g}.

TABLE II
N → V TRANSITIONS IN ANTHRACENE

Transition	Description	Excited confign	Polarization
N → V_1	$R_2^2 \rightarrow R_2P_3$	B_{2u}	y
N → V_2	$Q_2^2 \rightarrow Q_2P_3$	B_{3u}	x
N → V_4	$R_1^2 \rightarrow R_1P_3$	B_{2u}	y

C. OTHER LCAO CALCULATIONS

There have been a number of attempts to make the molecular orbital treatment more sophisticated. Pariser (90) used a theory based on the LCAO approximation which includes interaction between the configurations forming the excited states. Furthermore Pariser adjusted some theoretical quantities by empirical or semiempirical procedures to make the theory more practicable. His calculations confirm previous results as well as predict a number of highly excited states. In a more recent investigation (93) similar results are obtained using self-consistent field molecular orbitals and only limited configuration interaction instead of the extensive configuration interaction and "crude" orbitals of Pariser.

Theoretical results similar to those already discussed are obtained by Dewar and Longuet-Higgins (42) and Pople (98). These calculations include triplets. Some of Pople's results for anthracene are contained in Table III. The second transition is predicted to be very weak and close to the intense first transition, so that it is very difficult to separate them experimentally. The theoretical levels are seen, however, to be in qualitative agreement with experiment.

TABLE III

TRANSITIONS IN THE ANTHRACENE MOLECULE

Excited config	Frequency, cm^{-1} Theoret	Frequency, cm^{-1} Exptl	Excited config	Frequency, cm^{-1} Theoret	Frequency, cm^{-1} Exptl
$^1B_{2u}$	30,000	26,500	$^3B_{2u}$	18,000	14,700
$^1B_{3u}$	33,500	(28,000)	$^3B_{3u}$	32,000	...
$^1B_{3u}$	45,500	39,000	$^3B_{3u}$	33,500	...
$^1B_{2u}$	52,000	45,500	$^3B_{2u}$	43,500	...

D. THE PERIMETER MODEL

A method which is quite frequently used to label molecular states is that of Platt (64, 96) who uses a free electron "perimeter" model. The method assumes that the π electrons of planar conjugated systems are free to move along the bonds throughout the system. The classification of π orbitals is like that of the orbitals of a free electron traveling in a one-dimensional loop of constant potential around the perimeter. The perimeter free-electron orbitals and their energies are calculated by distorting the perimeter into a circle of the same circumference and assuming this system to correspond to a plane rotator so that the energies are

$$E = q^2h^2/2ml^2 \qquad \text{(Eq 3)}$$

where q = an integer 0, 1, 2, ..., h = Planck's constant, m = electronic mass, l = length of perimeter (in angstroms), and E = energy in reciprocal centimeters. It can be seen from Eq 3 that the energy levels are quadratically spaced and are doubly degenerate (except for the lowest with $q = 0$), since electrons may travel either clockwise or counterclockwise around the loop. The total momentum number $Q = \Sigma q$ may take on values 0, 1, 2, ..., and such states are designated by A, B, C, ... When Q takes on values $2n$, $2n + 1$, $2n + 2$, ... for systems with n benzene rings, these states are identified by K, L, M, ..., irrespective of the value of n. The highest filled level has $q = n$, and the four electrons in this level are called f electrons, those in the level immediately below e electrons, and so on. The first empty level has $q = n + 1$ and is called the g level, the one above the h level, and so on.

The electrons have been assumed to move under the influence of a potential which, to a first approximation, is constant, resulting in doubly degenerate excited states. Since the potential is provided by the atoms of the benzene ring, it follows that the potential is not constant but periodic. This fact, together with the inclusion of the effects of the cross-links between atoms 3,10 and 5,12 of Figure 3, removes the degeneracy. Each state thus splits into two components which are labeled by subscripts a and b.

The most important transitions are those from a filled to an empty shell. Spectra produced by the excitation of two electrons will be weak and will require higher excitation energies. For a transition from an f to g level, the new states are

$$Q = (n + 1) \pm n = 1 \text{ or } 2n + 1$$

which are B and L states, respectively. On removing the degeneracy these become B_a, B_b, L_a, L_b, and since electron or hole spins may be parallel or anti-parallel each can be either singlet or triplet, giving a total of eight possible states for the f^3g configuration.

Platt's model has been extended by Moffit (81). This has enabled further calculation to be made, the results of which account for the more prominent features of the electronic spectra of cata-condensed hydrocarbons. Experimental results of McClure (77) on the polarization of π-electron transitions in aromatic molecules agree with the predictions of the perimeter model, certainly for the lower excited states. The first three allowed singlet states are L_a, L_b, and J_a, respectively, corresponding to the three transitions described in Table II.

IV. CRYSTAL ENERGY LEVELS

A. FIRST-ORDER THEORY

The most satisfactory description of the crystalline energy states of aromatic substances thus far produced is that based upon the "exciton" or nonconducting excited states (47, 48, 94). This concept enabled Davydov (40) to determine theoretically the energy levels of anthracene-like molecular crystals using what might be called a weak-coupling model in which the interaction energy between molecules is assumed to be small compared with the intramolecular energy. This work has been extended by Craig and Hobbins (36–38).

In this exciton migration model the unperturbed state can be represented by a collection of molecules which are not interacting with each other. If the Schrodinger equation is used to describe the energy levels of the kth molecule, then the ground state of the crystal is written, following the assumption of weak coupling, as a simple product of molecular wave functions of the collection of N unexcited molecules. A set of excited states is obtained by assuming that if the collection of molecules were separated from each other by an infinite distance, $N - 1$ of the molecules would be in the ground state, the other (the pth, say) would contain the energy of excitation.

The molecules in the crystal do interact with each other slightly, and to represent this interaction a small term, the interaction potential V, must be included in the unperturbed Schrodinger equation. This potential operator has the full symmetry of the crystal lattice so that the wave functions must also have this symmetry. Since the interaction is in this instance a purely crystalline phenomenon, we have here the first effect of the crystalline field on the molecular states.

The energy levels E and wave functions Φ of the crystal are defined by the equation

$$\sum_{k+1}^{N} (H_k + \sum_{l>k} V_{kl})\Phi = E\Phi$$

According to first-order perturbation theory, the energy of the ground state is

$$E_G = \sum_{k=1}^{N} \omega_k + \Sigma\Sigma\int \zeta_i\zeta_k V_{ik}\zeta_i\zeta_k \, d\tau \qquad \text{(Eq 4)}$$

where ω_k is the isolated energy of the kth molecule in the ground state described by the antisymmetric wave functions ζ_k. Primed quantities would indicate an excited molecule.

It follows that the crystal wave function is

$$\Phi_r = \sum_{l=1}^{N} a_{rl}\phi_l$$

where

$$\sum_{l=1}^{N} a_{rl}^* a_{rl} = 1$$

Φ_r is one of N crystal excited states all belonging in the weak coupling model to the excitation of one molecule to an excited state. The quantity $a_{rp}^* a_{rp}$ is the probability that the pth molecule is the excitation "site." When N is large the coefficients differ from one another only in their phase factors, and may be obtained from the usual secular equation

$$\det|(\Sigma H_k + \Sigma\Sigma V_{kl})_{pq} - \delta_{pq}E| = 0$$

The diagonal elements can be written

$$\int \phi_p^*(\Sigma H_k + \Sigma\Sigma V_{kl})\phi_p \, d\tau - E \qquad \text{(Eq 5)}$$

Since ϕ_p is the wave function of the zeroth approximation to the crystal excited state for which the excitation is located at the pth molecule, it is seen that for the diagonal elements the excitation is localized at this pth molecule. Remembering this when we use Eq 4 in Eq 5 we get for the diagonal elements

$$\sum_k{}'\omega_k + \omega_p' + \sum_k{}'\sum_{l>k}{}'\zeta_k\zeta_l|V_{kl}|\zeta_k\zeta_l + \sum_l{}'\zeta_p'\zeta_l|V_{pl}|\zeta_p'\zeta_l - E \qquad \text{(Eq 6)}$$

where the primed sum indicates that the excited (pth) molecule has been omitted.

The nondiagonal elements are of the form $\int \phi_p^* \cdot (\Sigma\Sigma V_{kl})\phi_q \, d\tau$. Since for these elements $p \neq q$, the excitation is not localized on a particular molecule, and the expression similar to Eq 6 for nondiagonal elements is

$$I_{pq} = \zeta_p'\zeta_q|V_{pq}|\zeta_p\zeta_q' \qquad \text{(Eq 7)}$$

The excitation can be said to have transferred from molecule p to molecule q under the influence of the interaction potential. This is the exciton. Equation 7 is an expression for the exciton "exchange" integrals for an exciton hopping for the pth to the qth molecule.

The magnitude of the energy transferred in this way is obtained by subtracting the ground-state energy (Eq 4) from the diagonal elements of the energy matrix. This gives a secular equation whose roots are the crystal excitation (exciton) energies. If in particular only the pth elements are considered, we obtain from this subtraction

$$\Delta\omega_p + D - \Delta E \qquad \text{(Eq 8)}$$

where $\Delta\omega_p = \omega_p' - \omega_p$ and

$$D = \sum_l{}'\{(\zeta_p'\zeta_l|V_{pl}|\zeta_p'\zeta_l) - (\zeta_p\zeta_l|V_{pl}|\zeta_p\zeta_l)\}$$

B. THE INCLUSION OF SYMMETRY

The molecular wave functions must be combined in such a way that these combinations transform like representations of the unit cell group. The relations between representations of the molecular group D_{2h} and the unit cell group C_{2h} are included in Table IV (37).

TABLE IV

REPRESENTATIONS OF THE UNIT CELL GROUP C_{2h}

	E	C_{2h}	i	σ_b	Associated D_{2h} representation
A_g	1	1	1	1	A_{1g}, B_{1g}
A_u ($\vec{r}_b$)	1	1	−1	−1	B_{2u}, B_{3u}
B_g	1	−1	1	−1	A_{1g}, B_{1g}
B_u ($\vec{r}_a$)	1	−1	−1	1	B_{2u}, B_{3u}

Unit cell wave functions γ are now defined, corresponding to the excitation of the two molecules (identified by subscripts 1 and 2) in the unit cell individually.

$$\gamma^{\alpha,\beta} = 2^{-1/2}(\phi_1 \pm \phi_2)$$

The α- and β-unit cell functions formed by combining the g-type molecular wave functions transform like the A_g and B_g crystal species, respectively, those from B_{2u} and B_{3u} molecular functions like B_u and A_u. Combining the $\gamma^{\alpha,\beta}$ into a form which must transform like a representation of the space group gives

$$\Phi^{\alpha,\beta}(\vec{k}) = (N/2)^{-1/2}\sum_f^M [\exp(i\vec{k}\cdot\vec{r}_f)]\gamma^{\alpha,\beta}(\vec{r}_f) \qquad \text{(Eq 9)}$$

where $\vec{r}$ is a lattice translation with components a, b, and c and $k_a = 2\pi\sigma/M_a a$ for $\sigma = 0, \pm 1, \pm 2, \ldots, \pm M_a/2$. σ numbers the M_a cells along the a axis, and k_a is a wave vector of the reciprocal lattice. Similar results obtain for the b and c directions.

C. APPLICATION OF THE SELECTION RULES

The selection rule for the wave vectors may be deduced from the transition dipole moment integral for the transition from the ground state Φ_G to the excited states $\Phi^{\alpha,\beta}$. It can be shown that this transition moment vanishes unless $\vec{k} = 0$. This selection rule applies to the rigid lattice. The band width may become finite on account of the excitation of lattice vibrations, although even then the transitions for which $\vec{k} = 0$ are still the most intense.

This transition rule means that of the manifold of levels described by Eq 9 only two are effectively excited. Thus from starting with a single molecular electronic level, we now have two levels in the crystal, corresponding to

$$\Phi_G \rightarrow \Phi^{\alpha,\beta}(0) \qquad \text{(Eq 10)}$$

A further selection rule is obtained from the fact that, since the unit cell has a center of symmetry, only g → u transitions are allowed from the ground state, as is the case with a single molecule. It follows that only those transitions are allowed which correlate with allowed molecular transitions, and their polarization may be read from Table IV. Thus crystal transitions related either to molecular transitions $A_{1g} \rightarrow B_{2u}$ (short axis polarized) or $A_{1g} \rightarrow B_{3u}$ (long axis polarized) have their α components polarized in the ac crystal plane and their β components along the b crystal axis.

D. DAVYDOV SPLITTING

It is found that the α and β crystal states corresponding to a given molecular state not only are polarized in different directions, but have different energies. The difference in energy is called the Davydov splitting and is caused by the exchange interaction of molecules which are not translationally equivalent, *i.e.*, of the different molecules of a unit cell. The exchange interaction of molecules which are translationally equivalent simply displaces the spectrum of the crystal relative to that of the free molecule. If I_1 is the exchange interaction term for translationally equivalent molecules and I_2 the term for molecules not translationally equivalent, then

$$I_1 = \sum_p I_{lp} \text{ and } I_2 = \sum_m I_{lm} \qquad \text{(Eq 11)}$$

where p runs over molecules translationally equivalent to the lth molecule and m runs over the others. The exciton Coulomb term D of Eq 8 also contributes to the displacement of the crystal lines or bands relative to those of the free molecule. Thus the energy of the transition from ground to crystal excited state can be written

$$\Delta E^{\alpha,\beta} = \Delta\omega + D + I_1 \pm I_2 \qquad \text{(Eq 12)}$$

The upper sign refers to the α wave functions, the lower to the β. The Davydov splitting is equal to $2I_2$. It differs from the usual splitting of levels in crystals in that it occurs even for molecular states which are not degenerate. Since it is brought about by the wandering of excitation energy in the crystal, it is confined to the excited states.

E. SECOND-ORDER EFFECTS

Craig (36) has shown that the effect of second-order perturbations on weak transitions is not negligible. The effect is particularly noticeable when a strong molecular transition is found near the weak one. Then intermolecular forces bring about interaction between the strong upper state of one molecule and the weaker upper state of a neighboring molecule, leading to intensity stealing. Under these conditions the second-order effects become comparable with those of the first-order.

Quantitatively, Craig shows that the intensity transfer should be most noticeable when the weak system is 0.1 to 0.2 times as strong as the intense one, and greatest in the crystal direction in which the strong transition has its major component.

F. VIBRONIC LEVELS

Vibronic wave functions $\zeta^r \cdot \sigma^{r(n)}$ can be written for the rth excited electronic state, where $\sigma^{r(n)}$ is the vibrational function corresponding to the nth quantum state of the vibration. In general the vibration differs from one electronic state r to another. For the less complex aromatic compounds, however, there is a simplification of both the second-order perturbation and the vibrational energy problems in that there is usually only one very intense system. Therefore the energy-level systems can be considered to consist of a weakly excited first upper state ζ^1 with a progression of vibrational sublevels, and an intensely excited second upper state ζ^2 without vibrational structure, plus further upper states ζ^r.

In anthracene vapor spectra, ζ^1 is found to have up to five members of the vibrational progression with a mean spacing of 1400 cm^{-1} between successive sublevels. The spacings are very nearly equal for both vapor and solution spectra, but in the crystal the intervals are distorted and differ along the a and b directions. The Davydov splittings are also found to differ from sublevel to sublevel. However, since the Davydov splitting is small for this the first band, the differences in splitting are neither very noticeable nor very certain, different crystal specimens of anthracene giving different results.

V. EXCITONS

A. CHARACTERISTICS OF THE EXCITON

The exciton not only plays an important part in shaping the ultraviolet properties of anthracene, but is itself an interesting subject of study. We have seen that excitons correspond to the "hopping" of the crystal energy of excitation from one molecule to another since the localization of the excitation state in a particular molecule does not correspond to a stationary state of the crystal as a whole. The stationary state is obtained by allowing the excitation state to be delocalized over all molecules of the same kind in the form of an excitation wave. This type of exciton is called a Frenkel or molecular exciton. However, Wannier

(116) and Mott (83), who were concerned with the optical properties of semiconductors, view the exciton as a conduction band electron and a valence band hole which are bound together and traveling through the crystal, although they may be separated by an appreciable distance. This type of exciton is usually called the Wannier–Mott exciton.

Knox (65) has pointed out that these two views are not as unrelated as they may seem. Since an excited atom can be described essentially as an electron bound closely to an ion by the Coulomb interaction, the two excitons differ physically merely in their "radii," *i.e.*, in the degree of separation of the electron and hole. Frenkel's case corresponds to a tight-binding, Wannier–Mott's to a weak-binding approximation. The absorption spectra of ionic crystals, and particularly the alkali halides, are interpreted in terms of an exciton which has binding intermediate between the Frenkel and the Wannier–Mott. Knox summarizes the experimental evidence which provides a striking verification of the validity of the three approximations.

If an exciton is produced by the absorption of an incident photon, the initial wave vector of the exciton will be the same as that of the photon since momentum must be conserved. In this case, since the electric vector of the photon is perpendicular to the direction of propagation, the dipole moment of the exciton will be perpendicular to the wave vector $\vec{k}$, so that all excitons formed in this way are transverse. Interaction of the exciton with lattice vibrations or imperfections can cause it to be scattered, and such a scattering process can change a transverse to a longitudinal exciton and *vice versa*. It has been shown (76) that the transverse exciton energy increases with $\vec{k}$ so that the effective mass for this exciton is a positive quantity. The reverse is true for longitudinal excitons. The importance in this variation of the exciton characteristic lies in the fact that the exciton with negative effective mass has a smaller chance to decay radiatively. This point is discussed more fully by Davydov (41).

Davydov distinguishes between two limiting cases of the excitation wave: (1) free excitons—the transfer of the exciton from one molecule to another is much more rapid than the intramolecular vibration frequencies, so that the change in the forces of interaction between neighboring molecules when one molecule in the crystal is excited cannot displace the molecules to a new equilibrium position before the exciton has transferred; (2) "localized" excitons—the excitation propagates much more slowly than the intramolecular vibration frequency so that the molecules do have time to occupy new equilibrium positions before the exciton can move. The progress of the exciton is impaired since local deformations arise in the crystal.

It can be shown that the "localized" excitons do not correspond to stationary crystal states and that spontaneous emissions take place into states in which all the excitation is distributed over the lattice vibrations. Thus there is little likelihood of radiative emission from a "localized" exciton. This is important since an exciton, originally free, may become "localized" through interactions with phonons, defects, impurities, or surface molecules during its diffusion through the crystal.

B. DECAY

There are basically two ways in which the energy of excitation of the crystal can be transformed (assuming no photochemical reaction to take place) after a photon has been absorbed. It can either be degraded to heat or reradiated as electromagnetic waves. Since the two processes are not mutually exclusive the luminescence is usually of a lower energy than the incident radiation. Transformation of excitation energy to heat may be by direct conversion into lattice vibrational energy or the excitation may suffer intramolecular conversion to vibrational energy of the atoms which make up the molecule. The latter process has been called intramolecular deactivation.

Most organic crystals have luminescence spectra which are independent of the energy of excitation, the fluorescence being observed to originate from the lowest excited singlet state of the molecule. It is obvious then that the nonradiative transformation of the excitation from higher to this lowest excited state must take place much more rapidly than the natural decay of the higher excited states which have half-lives of 10^{-10} to 10^{-11} sec. Hochstrasser (52) argues that since the quantum yield of fluorescence from these higher states is negligible, the nonradiative decay of excitation energy must have a half-life of the order 10^{-12} and 10^{-13} sec. Similar values have been estimated experimentally by other means (113). This process of nonradiative decay to the lowest excited state is called internal conversion and is extremely efficient for anthracene.

If the probability that a given exciton luminesces is denoted by P_l, that it transforms to a "localized" exciton by P_t, that it decays to lattice vibration by P_v, and that it suffers intramolecular deactivation by P_d, then the ratio η of the number of excitons emitting their energy as luminescence to the total formed is

$$\eta = \frac{P_l}{P_l + P_v + P_t + P_d} \qquad \text{(Eq 13)}$$

Each of the variables in Eq 13, as well as the implementation of the equation itself, is treated fully by Davydov (41).

The luminescence will decrease as the temperature rises since the number of free excitons will drop as the result of enhanced thermal transfer to "localized" states and to lattice vibrations. The same end result is obtained (8) if the crystal is allowed to oxidize or if the surface is damaged by radiation or abrasion. This

process is discussed in more detail in section IX. Similar results are obtained for 2-aminoanthracene in alcohol solution (117).

C. TRAPPING

Self-trapping of the exciton can result from large exciton–phonon coupling and makes itself apparent in the localization of the excitation at some definite site in the lattice, followed usually by nonradiative decay. Trapping can also take place at a crystal defect which has a sufficiently large capture cross-section, or at a crystal surface. This may occur without strong phonon coupling. The experimental evidence for these phenomena has been reviewed by Knox (65).

Sidman (104) believes that his interpretation of the gap between the anthracene absorption and fluorescence origins in terms of trapped excitons constitutes evidence for the trapping of excitons. He shows semiquantitatively that it is possible for trapped excitons to exist in anthracene: there is a shift of -2140 cm^{-1} of the 0–0 band of the lowest $A_g \rightarrow B_{2u}$ transition in the crystal relative to the vapor. The Coulomb exciton term D and exciton exchange energy I of Eq 12 are responsible for the shift. The necessary condition for the trapping of the exciton is $|D| >> |I|$, where $I = I_1 + I_2$. Sidman quotes calculated values of I and D as -650 and -1490 cm^{-1}, respectively, so that the condition for the trapping of excitons in anthracene is met theoretically. However, the existence of the gap between the first strong absorption and the fluorescence origin is open to doubt (4). Absorption and luminescence spectra measured on highly purified crystals at 4°K indicate that the absorption spectrum of anthracene is relatively simple and that there is no energy gap in the purest crystals.

D. SCATTERING

Excitons can be scattered by phonons, point defects, dislocations, and surfaces. The mean free path of excitons as defined by scattering with acoustic phonons has been investigated theoretically, and Knox (65) gives an expression for this path. Such a path for an exciton in a simplified model of anthracene has been estimated (1) to be 20 μ. It is found that the exciton diffusion coefficient is 1 cm^2 sec^{-1} which exceeds measured values by more than an order of magnitude. The discrepancy is ascribed to the role played by "localized" excitons, the presence of lattice defects, and the approximate nature of the calculation. Knox discusses qualitatively, giving references to further work, the scattering by dislocations and surfaces.

E. DIFFUSION

Early evidence for the diffusion of excitation energy within crystals was obtained from the fluorescence spectrum of anthracene which had a trace of naphthacene impurity introduced into it (49). In the pure crystalline state naphthacene hardly fluoresces, whereas dissolved in solid anthracene it fluoresces brilliantly with its characteristic yellow-green color, the host crystal fluorescence being quenched. Since the proportion of naphthacene molecules in the mixture is negligible, it is obvious that the initial absorption of light must be by the host crystal. The excitation is then transferred to the impurity where the excitation decays, giving the fluorescence characteristic of the impurity. Northrop and Simpson (87) have performed experiments on the efficiency of fluorescence transfer in solid solutions and find most of the results can be explained by a simple theory of exciton migration. In view of the small number of impurity molecules present it is clear that a simple process of reabsorption and reemission of the fluorescence cannot account for the effects (78).

Simpson (109) has attempted a direct measurement of the diffusion of excitons in anthracene. The basis of his experiment is the fact that a phosphor containing luminescence centers can be used as a detector of excitons. This makes it possible to detect the diffusion of excitons from an activator-free crystal into a contiguous crystal containing centers capable of trapping the exciton. Naphthacene-doped anthracene was used as the detector.

One surface of a thin anthracene specimen was covered with the detector and the opposite surface illuminated in the fundamental absorption band. The luminescence emitted by the detector is due partly to excitation by those incident photons which are not absorbed in the specimen and partly due to excitons which are formed in the specimen and diffuse to the detector where they are trapped and fluoresce. The two contributions are separated by a measurement of the transmission of the specimen alone so that the flux of excitons into the detector can be determined. It is assumed that the motion of the excitons can be described by the ordinary diffusion equation including terms for the creation and decay of excitons. This equation is solved using boundary conditions which fit the assumptions that (i) there can be no transport of excitons across the front surface which is free and (ii) the detector in contact with the back surface is a perfect absorber of excitons.

The agreement between theory and experiment is good. Simpson finds that when a diffusion length of $L = 460$ A is used in the solution of the diffusion equation, the theoretical exciton flux compares well with the measured transmission associated with the excitons. Regarding the motion of the exciton as a random walk allows this diffusion length to be used to obtain the displacement R

$$\overline{R^2} = 6D\tau = 6L^2 \qquad \text{(Eq 14)}$$

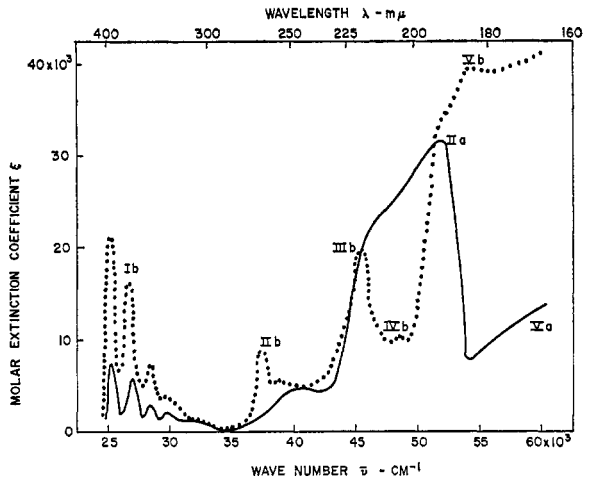

Figure 4.—The absorption spectrum of anthracene. The solid curve is the *a* spectrum, the dotted curve the *b* spectrum (19, 75).

giving a root-mean-square displacement between the points of origin and decay of the exciton of 1120 A. The mean number of steps in the absence of impurities will be 10^5 and the mean free path of the exciton 0.2 μ.

F. TRIPLET EXCITONS

Measurements on the diffusion of triplet excitons in anthracene have been made recently (119), the results yielding a diffusion coefficient (0.2–1.0) $\times$ 10^{-2} cm^2 sec^{-1} and a diffusion length 70–150 μ in a direction perpendicular to the *ab* plane. The thickness of the crystal was found to have a marked effect on the lifetime of the triplet state. A similar value for the diffusion coefficient has been reported elsewhere (61), although measurements which involve a different experimental technique (6, 68) show values for the diffusion coefficient about two orders of magnitude smaller. The implications of this discrepancy have been discussed (68). Reviews of earlier work on the triplet state in general (71) and on the role played by triplets in energy transfer in solution (118) have recently appeared.

VI. ABSORPTION

We have seen that the crystal states are derived from the molecular levels and that these are polarized either along the long or the short molecular axis. The change in levels which takes place in going from molecule to crystal is different for each of these polarizations. In addition the change depends on the intensity of the molecular transition so that the analysis of the experimental crystal spectrum in terms of the molecular states is in some instances uncertain. There are many experimental absorption spectra reported in the literature and Figure 4 is a composite of two of these spectra (19, 75). The experimental methods which have been used and the difficulties experienced in measuring such spectra have been discussed by Craig and Walmsley (39).

A. TRANSITION I

1. *Davydov Splitting*

The theory predicts that the first excited state in the molecule has symmetry B_{2u}, and in the crystal one should therefore see two components with small Davydov splitting, the intensity along the *b* axis being somewhat greater than along the *a* axis. That this is found experimentally can be seen from Figure 4. Craig and Hobbins (38) find that where Davydov splitting occurs for this transition it involves a *b* component displaced to lower frequencies and an *a* component to higher. They find that at $-140°$ the splitting is in the range 10 to 50 cm^{-1} which is compatible with a B_{2u} upper state but not a B_{3u}. They also establish that the interval between the second and third vibronic peaks is greater than that between the second and first (lowest energy) peaks, which is claimed to indicate an $A_g \rightarrow B_{2u}$ transition.

Sidman (104), who studied the spectrum at 4°K, was not able to confirm the splitting of vibronic states found by Craig and Hobbins. He found that the absorption maxima occur at the same energy in both *a* and *b* polarization to within the limits of his experimental error of ± 20 cm^{-1} which were set by the band width. The discrepancy may be resolved by studies (26, 78) which show that the spectra of both naphthalene and anthracene depend upon the strain to which the crystal is subjected. An examination of the absorption spectra of 23 anthracene crystals to see if the spectra were reproducible from one specimen to another showed (46) that the Davydov splitting of the absorption origin at 25,350 cm^{-1} amounted to as much as 60 cm^{-1} in some crystals and was practically zero in others having the same thickness.

It has been pointed out (22) than an inaccuracy of orientation of the light vector incident on the crystal along the *b* axis has a strong influence on the measured values of Davydov splitting. When special precautions were taken to eliminate this inaccuracy, larger Davydov splittings than those reported elsewhere were obtained, although different values were still found for different crystals. The mean values at 20°K for crystals ranging in thickness from 0.05 to 0.1 μ are 230, 145, and 80 cm^{-1} for the first three vibronic sublevels in increasing order of energy, respectively. Wolf (121) reports similar results.

2. *Polarization Ratios*

The polarization ratio, which is taken here to be the ratio of the area under the *b*-axis to the *a*-axis absorption curves, was found by early experimenters to be

about 2. When more care was taken with the polarization of the incident light in the experiments (121), the ratio was found to be about 3, and more recently (22) the ratio has been measured for the first three vibronic sublevels of this transition individually, the ratios obtained being 5, 4.5, and 3.2 in increasing order of sublevel energy, respectively. If the crystal is thought of as an oriented gas in which there is no interaction between the molecules, the calculated value for the ratio is 1/16 and 7.7 for transitions which are respectively long- and short-molecular axis polarized. More refined calculations which include second-order effects (39) yield ratios of about 1/2 and 3 for long- and short-axis polarizations, respectively, indicating that this crystal state has its origin in a short-axis polarized transition.

3. *Oscillator Strengths*

The formula for finding the reduced oscillator strength is

$$f_{a,b,c'} = 1.44 \times 10^{-9} \int \epsilon_{a,b,c'} \, d\bar{\nu} \qquad \text{(Eq 15)}$$

where $\bar{\nu}$ is in cm^{-1}, ϵ is the molar extinction coefficient, and c' is an axis at right angles to the a and b crystal axes. If this formula is used, then $f_a + f_b + f_{c'}$, should be approximately equal to the oscillator strength for the transition in solution, f_s. Table V lists the values of f_a and f_b reported in the literature together with the experimental method used in each case.

The solution oscillator strength is $f_s = 0.10$, so the figures in Table V imply $f_{c'} = 0.01$. Theoretical calculations (19) show that a B_{3u} upper state would have $f_{c'} > f_a, f_b$, but a B_{2u} upper state would have $f_{c'} = 0.01$, lending further support to the B_{2u} assignment.

TABLE V
OSCILLATOR STRENGTHS FOR TRANSITION I

f_a	f_b	Method	Ref
0.015	0.033	Direct absorption	14
0.025	0.064	measurements	19
0.017	0.04		23, 62
0.057	0.10	Extrapolation of	89
0.013	0.057	refractive indices	43
0.025	0.06	Reflection	14

A possible explanation for the widely varying values of oscillator strengths is found in the measurements (24) of the absorption coefficient at 20°K which show that the coefficient depends markedly on the thickness of the crystal. Decreasing the crystal thickness from 0.40 to 0.16 μ increases the absorption coefficient at the first vibronic peak by almost a factor of 2. Absorption curves measured at room temperature over the same range of thickness proved to be independent of thickness. A similar low-temperature effect is reported elsewhere (46). The variation of the absorption with thickness has been associated with the effects of spatial dispersion which will be discussed in section VII.

B. TRANSITION II

Transition II occurs in solution at about 250 mμ (56) and does not have the well-defined vibrational progression of transition I. This is a very intense transition, the oscillator strength being reported to be 2.3 in solution (38) and 1.6 for the vapor (75). Using $f = 2.3$, calculations show (37) that the Davydov splitting should be 16,000 and 1,000 cm^{-1} for B_{3u} and B_{2u} upper states, respectively. The crystal absorption spectrum shows a maximum at 268 mμ in b polarization, and, since this state has been assigned (section III) to be B_{3u}, the corresponding maximum in a polarization should appear at about 190 mμ. The intense peak appearing at roughly this wavelength in a polarization in Figure 4 has been taken, therefore, to be the a component of transition II. Comparison of crystal and solution extinction coefficients (19) confirms the assignment of system II to a B_{3u} upper state.

C. HIGHER TRANSITIONS

The b component of transition III is clearly seen in Figure 4 at 221 mμ. The experimental oscillator strength is $f_b = 0.16$ (18), while theoretically values of 0.005 and 0.2 for long-axis (B_{3u}) and short-axis (B_{2u}) polarizations are obtained (75). Thus the transition is probably to a B_{2u} upper state. This agrees in polarization with the assignments of Ham and Ruedenberg (50) of the state to ^1B_a in perimeter model notation and of Pariser (90) to the state (in his notation) B_{1u}^+ which is similar to our B_{2u}. Platt (96) has assigned the transition to the ^1C_b, which is forbidden in the molecule. Since the upper state is probably B_{2u}, the splitting should be small and the a component found near the b. This a component is probably hidden under and enhanced by the strong a component of transition II, which would account for the unusual shape of the a component in the region 190–220 mμ.

The small peak in the b spectrum at 207 mμ is taken by Lyons and Morris (75) to be the b component of transition IV which they consider to be long-axis polarized with the a component buried under the nearby strong a absorption. Pariser (90) predicts a transition with this polarization and of approximately the intensity observed to lie at 170 mμ. There is no clear-cut indication of an electronic transition in the solution spectrum in this region (55), and it cannot be stated with certainty that this is, in fact, an electronic transition.

Transition V is intense in solution with an oscillator strength $f_s = 0.4$, and appearing, from the crystal spectrum in Figure 4, to have its major component along the b axis, with f_b comparable with f_s. This would indicate a B_{2u} upper state although extrapolation from

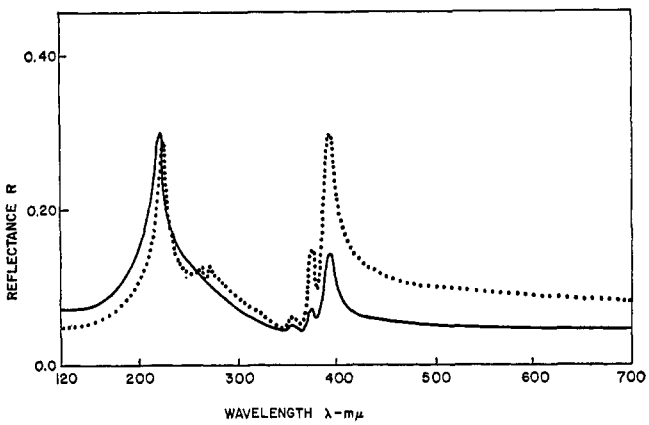

Figure 5.—The reflection spectrum of anthracene. The solid curve is the *a* spectrum, the dotted curve the *b* spectrum (128).

the free molecule to crystal states becomes uncertain at energies as high as this.

VII. Reflectivity and Optical Constants

A. Reflectivity

The reflection spectrum of anthracene along the *a* and *b* axes is shown in Figure 5, the wavelength range being from 120 to 700 mμ, although only that part of the spectrum between 220 and 400 mμ was measured (128). The remaining parts were calculated as described in section VII.B. The measurement was made at an angle of incidence of 20°. The reflection spectrum between 220 and 400 mμ has also been reported elsewhere (19). There is no significant difference between the two reported spectra. It can be seen from Figures 4 and 5 that the reflection follows the absorption spectrum quite closely, especially where the absorption is high. For example, the *b* component of transition II occurs at 268 mμ in the absorption spectrum and has its counterpart at 270 mμ in the reflection spectrum. In addition there is very little shift in the vibronic peaks of the first transition between the spectra.

Reflection spectra for the (001), (010), and (1′00) spectra, using unpolarized incident light, have also been made (126). (The (1′00) face is in the plane lying at right angles to the (001) and (010) crystallographic planes; it is not a true crystallographic face.) The unpolarized spectra for the (001) and (1′00) faces resemble quite strongly the *b*-polarized spectrum while that for the (010) face shows the vibrational progression of the first transition only very weakly. These results are to be expected since the *b* axis lies in the (001) and (1′00) faces.

It has also been shown (126) that ultraviolet irradiation for a period of several hours reduces the reflectivity slightly, while abrasion or aging in air reduce it markedly. It is assumed that all these agents enhance the oxidation of the crystal surface (44, 69) which is responsible for the reduction in reflectivity. Crystals which have been aged in the atmosphere for a period of 1 year or more, and presumably have an appreciable layer of oxides on the surface, show a different reflection spectrum from freshly cleaved specimens. A pronounced peak appears at about 250 mμ while the long wavelength reflectivity is unaltered. Anthraquinone has an intense absorption band near 250 mμ (105, 106) while being very nearly transparent at the longer (340 to 400 mμ) wavelengths. It has been assumed that the pronounced peak is caused by the surface layer of anthraquinone while at the longer wavelengths the reflectivity remains characteristic of the bulk material since anthraquinone is transparent in that region.

B. Optical Constants

1. *Reflection Method*

It is difficult to measure the ultraviolet optical constants of substances like anthracene by conventional transmission methods because they are so highly absorbing in this spectral region. The obvious recourse is to reflection methods, but in the case of anthracene these also present problems because the crystal is biaxial. Since two constants are to be determined (real and imaginary parts n and k of the refractive index), at least two independent measurements are required in the conventional reflection techniques (7, 108, 115). The anisotropy of the crystal means, however, that these two measurements correspond in general to a different pair of constants so that it is not possible to obtain a unique solution for these constants. The method of Price–Robinson (100, 101) has recently been extended (128) to solve this problem.

This method uses the Kramers–Kronig dispersion relation (82, 114) to calculate the imaginary part of the reflected light amplitude as a function of frequency from the real part which is measured. Knowledge of the real and imaginary parts of the reflected amplitude allows optical constants to be evaluated. In principle the method requires that the reflectivity be known at all frequencies, but in practice (17) it is found that the reflectivity spectrum need be known over a frequency range only somewhat larger than that over which it is desired to obtain optical constants.

The reflectivity spectrum has been measured between 220 and 400 mμ (19, 128) and extended to longer wavelengths (128) by calculating the reflectivity from refractive indices measured (43) between 400 and 700 mμ for both *a* and *b* polarizations. The extension to shorter wavelengths used the criterion (5) that the spectrum as a whole yields a phase which is everywhere positive and has a minimum at 283 mμ, the near-ultraviolet absorption minimum for anthracene. The complete reflectivity spectrum has been reproduced in Figure 5.

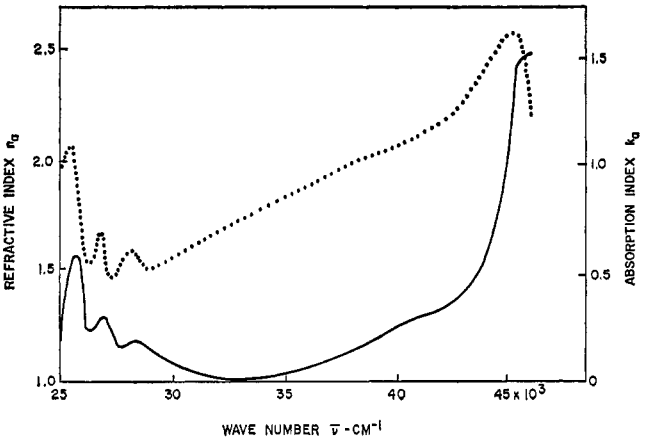

Figure 6.—The optical constants of anthracene along the a axis. The solid curve is the absorption index and the dotted curve the refractive index (128).

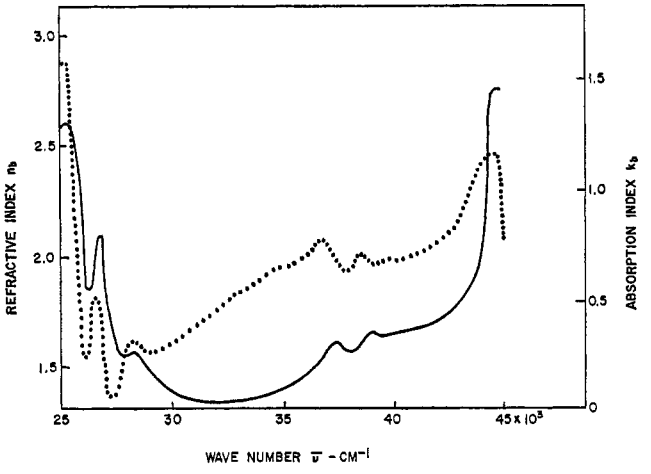

Figure 7.—The optical constants of anthracene along the b axis. The solid curve is the absorption index and the dotted curve the refractive index (128).

2. *Calculations of the Constants from Reflection*

The Kramers–Kronig relation which was used (128) had the form

$$\theta(\bar{\nu}_c) = -\frac{1}{\pi}\int_0^\infty \ln\left|\frac{\bar{\nu}+\bar{\nu}_c}{\bar{\nu}-\bar{\nu}_c}\right| \frac{d}{d\bar{\nu}}\left[\ln|r(\bar{\nu})|\right] d\bar{\nu} \quad \text{(Eq 16)}$$

where $\theta(\bar{\nu}_c)$ is the phase in radians at the particular wavenumber $\bar{\nu}_c$, and $|r(\bar{\nu})|$ is the magnitude of the reflected amplitude expressed as a function of wavenumber $\bar{\nu}$. The dispersion relation was applied to each of the reflection spectra R_a and R_b of Figure 5 to yield θ_a and θ_b, respectively, using Bode's method of solution (13). It has been shown (128) that if light is incident on the (001) face of anthracene with the (010) in the plane of incidence, then one electric displacement vector is in the plane of incidence, the other perpendicular to it. When these conditions are used in the usual method of deriving Fresnel's equation of reflectivity at normal incidence (15), the equation

$$r_l = \frac{n_l + ik_l - 1}{n_l + ik_l + 1} \quad \text{(Eq 17)}$$

is obtained, where l can be either the a or b axis. Since

$$r_l = |r_l| \exp(i\theta_l) \quad \text{(Eq 18)}$$

it follows that

$$n_l = \frac{1 - |r_l|^2}{1 + |r_l|^2 - 2|r_l| \cos\theta_l} \quad \text{(Eq 19)}$$

and

$$k_l = \frac{2|r_l| \sin\theta_l}{1 + |r_l|^2 - 2|r_l| \cos\theta_l} \quad \text{(Eq 20)}$$

The optical constants n_l and k_l calculated from Eq 19 and 20 are shown in Figures 6 and 7.

3. *Validity of Reflection Optical Constants*

Experiments have been performed (20, 21, 25) which show that the Kramers–Kronig relations possibly are not valid for the dispersion process in anthracene and related substances at low temperatures and at frequencies in the exciton absorption band. The invalidity is ascribed to the effects of spatial dispersion. A theory using the concept of spatial dispersion in the region of an exciton band has been developed (54) to obtain an expression for the reflectivity in this region. A radical departure from the shape of reflectivity peaks expected from the classical theory is found, the most striking aspect of the new peaks being very sharp subsidiary spikes. These spikes have been observed experimentally in the reflectivity spectra of CdS and ZnTe when the temperature is below 20°K. Above this temperature the reflectivity is that which is expected classically. It is concluded that spatial dispersion does not reduce the utility of Kramers–Kronig determinations of optical parameters near sharp exciton dispersion peaks since such determinations are related to effective optical parameters only. The optical constants shown in Figures 6 and 7 were obtained at room temperature and cover a much wider frequency range than the exciton band, and were therefore considered (128) not to be seriously affected by spatial dispersion.

4. *Optical Constants from Absorption*

The optical constants along the a and b axes in the first absorption band of anthracene have been measured by an absorption method at 20 and 293°K (23). The absorption indices are slightly higher at the lower temperature, although they are generally lower than those obtained from the reflectivity. The latter method, however, yielded refractive indices which were generally lower. Optical constants obtained by the absorption method show the same wavelength dependence as those in Figures 6 and 7, although they cover only the first absorption band.

VIII. PHOTOCONDUCTIVITY

A. EXPERIMENTAL METHODS

These are basically two types of cells which have been used to measure photoconduction in anthracene. In the surface cell two electrodes are connected to the same crystal surface, separated by a gap of 1 or 2 mm. This type of cell has given reasonably consistent results, and in particular it shows that the photocurrent plotted as a function of the exciting wavelength follows closely the crystal absorption spectrum (27, 28, 72). The other type of cell, the sandwich cell, has electrodes on opposite sides of a crystal which is typically 3 mm thick. Results with this type of cell have not been consistent. Thus there are reports that the photoconductivity excitation spectrum does not follow the absorption (66, 67) as well as those which find a close correspondence (112).

The discrepancies between different results can be attributed to several causes. In the first place the surface of the crystal has been shown to play a leading role in the formation of charge carriers in anthracene. Thus a large component of the photocurrent is a surface phenomenon, dependent critically on the surface condition of the crystal. A smaller component of the current, originating in the bulk of the crystal, is less dependent on crystal condition, and, since the different types of cells tend to favor measurement of one component over the other, disagreements arise.

Differences in electrodes are also thought to be the cause of discrepant results. The use of an electrolytic solution as an electrode (112), instead of the older conductive glass sheets or semitransparent metal electrodes, gives results in a sandwich cell which are in agreement with those of the surface cell. Pope (97) is of the opinion that most, if not all, of the energy difference between the fundamental absorption band energy and that needed for the production of charge carriers in the crystal is provided by an electrode–crystal interaction. In an investigation of the current–voltage relationship of anthracene photoconduction with a number of electrode systems (99), it is shown that the nonohmic behavior and the accompanying strong crystal polarization effects arise from large potential barriers near the electrode.

Anthracene is a very good insulator which is the reason why photoconductivity measurements are often marred by electrode and space charge effects. A measurement technique (58, 59) in which a pulse of light usually about 1 μsec long is transmitted through semitransparent electrodes not in contact with the crystal eliminates these problems. The electrodes provide a field of the order 1 kv cm^{-1} which causes the charge carriers produced in the crystal by the light pulse to drift. This drift results in redistribution of charge in the external circuit which can be observed on an oscilloscope, providing an indication of the number and drift mobility of the carriers.

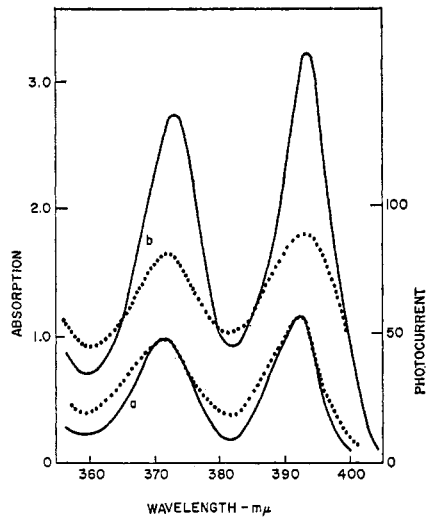

Figure 8.—The photoconductivity excitation spectrum of anthracene (dotted curves) and the absorption spectrum (full curves) (112).

B. THE EXCITATION SPECTRUM

Despite earlier variations (introduced mainly by electrode and space charge effects), it is now generally agreed that the relative quantum efficiency for the production of carriers as a function of the exciting light follows closely the absorption spectrum of the crystal. This can be seen from the excitation spectrum in Figure 8, which is the work of Steketee and de Jonge (112). This spectral dependence has been accounted for (72) by assuming that photoconduction is a surface phenomenon. Initially light is absorbed in the crystal and an exciton formed. This exciton diffuses throughout the crystal, and, if it reaches the surface, could produce a charge carrier there. The average distance of the point of origin of the exciton from the surface is determined by the wavelength of the exciting light. Thus, for a wavelength which is strongly absorbed, excitons are formed near the surface and have a high probability of reaching the surface and a high photocurrent is observed. This brings about the observed similarity between the excitation and absorption spectra.

Figure 8, which was obtained with a sandwich cell and electrolytic electrodes, has been analyzed in terms of the diffusion of excitons to the crystal surface where charge separation takes place. The diffusion equation, including terms for the creation and decay of excitons

$$\frac{\partial n(x)}{\partial t} = D\frac{\partial^2 n(x)}{\partial x^2} + \alpha I_0 e^{-\alpha x} - \frac{n(x)}{\tau} \quad \text{(Eq 21)}$$

was solved with the boundary conditions $n(0) = 0$ and $n(d) = 0$ where $n(x)$ is the number of excitons at a distance x from the illuminated face of the crystal, D the

diffusion coefficient in the x direction, τ the mean lifetime of an exciton, I_0 the photon intensity, α the crystal absorption coefficient, and d the crystal thickness. If the photocurrent is assumed to be directly proportional to the exciton flux through the interface between the positive illuminated electrode and the crystal, then the result of solving Eq 21 shows that the photocurrent is proportional to the absorption coefficient, which is observed experimentally. The mean free diffusion path $(D\tau)^{1/2}$ of an exciton is estimated to range from 700 to 2000 A for different crystal specimens of anthracene. Since the length of the diffusion path will depend on the amount and nature of impurities and imperfections in the crystal, this variation is not unexpected. These values for $(D\tau)^{1/2}$ are in agreement with those reported elsewhere (45, 109).

At wavelengths shorter than those shown in Figure 8, the resemblance between photoconductivity curves and the absorption spectrum apparently ceases (28), and it is thought that this might be due to some experimental failure since this region of the spectrum is very difficult to work in. On the long-wavelength side, photocurrents have been excited in anthracene by the 6943-A ruby laser line (51). At room and higher temperatures the currents are proportional to the square root of the intensity of the exciting light. This progressively changes to a linear relation as the temperature is lowered to $-25°$. The results do not support the contention (95) that a double-photon excitation of the first excited singlet state of anthracene has occurred, nor do they indicate exciton dissociation as the cause of the free carriers. Instead the observed photocurrents have been attributed to single photon excitation of anthracene ions or trapped carriers.

C. THE BULK PHOTOCONDUCTIVITY

The above interpretation of photoconduction in anthracene assumes that charge carriers are formed by the interaction of excitons with the crystal surface. There is, however, a body of experimental evidence which suggests that the photoconductivity is not entirely a surface phenomenon (66, 67, 73). In order to explain the existence of the small but definite bulk photoconductivity in anthracene, the possibility of obtaining ionized excited states as the result of light absorption has been examined (74). These states are estimated to lie at energy levels accessible to visible and ultraviolet light. Since the anthracene molecule has a positive electron affinity, the electron may be trapped at the nearest neighbor molecule and the conduction produced by the subsequent movement of the hole through the crystal. The term "separated exciton" has been coined to describe this situation.

An investigation (88) into the anthracene bulk photoconductivity using a technique of growing thin single crystals between glass flats, which avoids spurious space charge effects as well as surface photooxidation to which anthracene is very susceptible, yields results which are interpreted in terms of exciton–exciton interaction leading to molecular ionization. Further experiments (107) show that if exciting light is used which is weakly absorbed (and therefore excites those molecules lying well into the bulk crystal), then the photocurrent is proportional to the square of the intensity of the light. This indicates that a bimolecular process, such as exciton–exciton interaction, is taking place. In addition, the observed rate of carrier production is in agreement with that calculated (30, 31). For strongly absorbed light a unimolecular process must occur since the photocurrent is linearly related to the light intensity as has been widely observed. In this case the excitons are being formed close to the illuminated surface and the exciton–surface interaction is presumably responsible for the majority of the carriers. The reabsorption of fluorescence and the diffusion of excitons through the crystal will tend to mix these two carrier-producing processes.

Kearns (57) has examined theoretically three possible mechanisms of photoconduction in organic molecular crystals: the production of charge carriers as the result of (i) the interaction of two singlet excitons, (ii) the interaction of two triplet-state excitons, and (iii) the interaction of a singlet with a triplet exciton. Depending on illumination conditions and crystal purity it is found that any one of these may be the dominant mechanism for the generation of free carriers by a multiple exciton process.

Investigation into the production of charge carriers by exciton–exciton and by exciton–surface interactions (60) reveals that, as a result of the very high carrier production rate predicted for the exciton-exciton process, it is necessary to invoke some type of carrier recombination in order to reconcile theory and experiment. Examination of the direct electron-hole recombination process shows that while it can explain the observed carrier quantum yield, it cannot at the same time account for the experimental intensity and absorption coefficient dependence. Introduction of monomolecular surface recombination does, however, enable all data to be fitted to the theory.

D. THE EFFECTS OF IMPURITIES, DEFECTS, AND GASES

It has been found (86) that impurities which quench the fluorescence of anthracene greatly reduce the photocurrent, but that an impurity which leaves the fluorescence unchanged has no influence on the photoconduction. α-Particle bombardment (129), neutron bombardment (32), and abrasion (69) reduce both the photoconductivity and fluorescence efficiencies. From experiments like these in which like effects are noted on photoconduction and fluorescence excitation, it has been concluded (32) that these two phenomena are compet-

ing processes in the disappearance of the exciton. It has been suggested that the exciton disappears at a molecule located at a dislocation and that both the incorporation of impurities and extensive radiation localize the exciton and produce internal quenching of the fluorescence and photoconductivity.

The photoconductivity is found to increase in the presence of gases which are electron acceptors (*e.g.*, oxygen) and to decrease when the ambient gases are electron donors (102). The behavior in the presence of oxygen has been widely observed. If, after this increase in the presence of oxygen has been observed, the crystal is placed under hard vacuum, then the photocurrent is found to return to its original value. This indicates that the increase is due to an interaction with adsorbed oxygen molecules. It also indicates (and this has been deduced from other experiments as well) that the majority carries in anthracene are holes.

IX. FLUORESCENCE

A. EMISSION

The emission spectrum of anthracene lies almost wholly outside the ultraviolet, and for this reason will not be considered here in any great detail. There are three components to the emission: fluorescence, which will be discussed in this section and which corresponds to a radiative transition from the excited singlet states to the ground state; phosphorescence, which is a longer wavelength emission than fluorescence and has a longer decay time although the decay is exponential; and delayed fluorescence, which has the same spectrum as fluorescence but a longer, nonexponential decay. Phosphorescence and delayed fluorescence have recently been reviewed in some detail (71, 91).

The fluorescence originates from the first excited singlet state regardless of which absorption band is excited, indicating that internal conversion from the higher to the lowest excited state is very efficient. A mirror-image relationship between absorption and emission spectra (16, 92) shows that the vibronic sublevels of the ground and first excited states are similar. The relationship is more readily apparent (29) if the number of quanta emitted per unit frequency interval *vs.* frequency is plotted. This method of plotting has the further advantage that the area under the curve is directly proportional to the fluorescence efficiency of the substance which allows unknown quantum yields to be obtained from comparison with some standard. Inspection of the mirror-image relationships indicates a progressive red shift and increased separation of the 0–0 bands in going from vapor through solution to solid-state phases of anthracene.

Fluorescence spectra of both microcrystal and thick anthracene crystal have been measured (11) and from the results the degree to which fluorescence is reabsorbed in the crystal obtained. The reabsorption is quite significant because of the considerable overlap between the crystal absorption spectrum and the molecular fluorescence spectrum, the latter being assumed to be the same as the spectrum of the microcrystal. The reabsorption reduces the quantum efficiency from the molecular value 0.94 (11, 124) to a thick crystal value 0.79. The decay time of the fluorescence is also affected by the reabsorption (9), increasing from 10 nsec for a thin flake to 31 nsec for a thick crystal. The decay time is independent of thickness for a crystal more than a few millimeters thick if surface oxidation, which readily reduces it, can be avoided. Birks (8, 9) has summarized all reported values of the decay time and accounted for the variations by allowing for the effects of reabsorption and surface quenching of excitons.

The decay of the fluorescence of a thick crystal which has been freshly cleaved is a pure exponential (10) while that for a crystal with oxidized surfaces appears to have two exponential components. This finding is supported by a study (63) which shows that, if the effects of reabsorption in a nonhomogeneous medium, such as anthracene with a surface layer of oxides, are taken into account, the decay of fluorescence will be nonexponential. Reabsorption effects have also received general treatment elsewhere (2, 3, 80).

Detailed examination of the emission spectrum shows that it is very variable with experimental conditions (122), and it is clear that imperfections and impurities have a marked effect on fine structure within the spectrum. The emission is also sensitive to radiation damage (103) and abrasion (69) of the crystal, both of these treatments decreasing the fluorescent efficiency. γ-Ray irradiation of anthracene in air, vacuum, or helium atmospheres produces the same degradation of the emission showing that the change is not due to oxidation. Both intense ultraviolet irradiation and α-particle bombardment reduce the fluorescence output (12). The transfer of excitation in mixed crystals, a field of investigation in which anthracene is used extensively, has been reviewed recently by Birks (8) who also treats the use of anthracene as a scintillator in great detail. Energy transfer in solution (118) and solid state (120) have also been reviewed.

B. EXCITATION

The efficiency with which fluorescence is excited in anthracene has been measured as a function of the wavelength of the exciting light (123, 125) and found to have an inverse relation to the absorption spectrum, although the relationship is less clear-cut at shorter wavelengths. It is found that both aging or abrasion of the crystal surfaces reduce the excitation efficiency markedly, while at the same time the structure in the excitation spectrum becomes more pronounced. The dotted curve in Figure 9 is typical of measured excitation spectra.

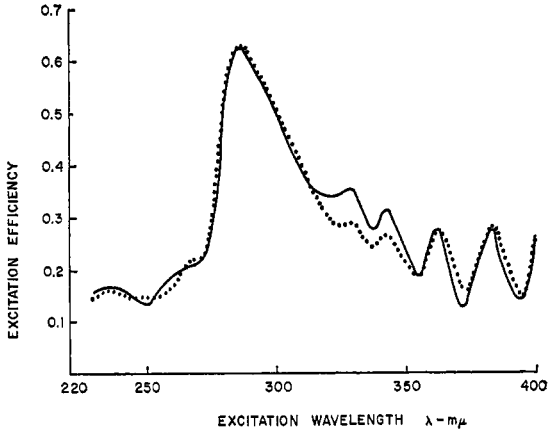

Figure 9.—Fluorescence excitation spectra of anthracene. The dotted curve is experimental, the full curve theoretical (127).

The variations in the excitation spectrum have been analyzed quantitatively (127) by assuming that they are principally the effect of a layer of anthraquinone which forms when the crystal is abrased or aged in the atmosphere. A model which takes into account selective absorption of incident radiation in this surface layer of anthraquinone, specular reflectance by the bulk crystal, quenching of the fluorescence *via* nonradiative exciton decay at the surface, and the absorption characteristics of the bulk crystal (including reabsorption and reemission of part of the fluorescence) was used to obtain a theoretical fluorescence excitation spectrum. This spectrum is the solid line in Figure 9. The agreement between the measured and the calculated spectrum is quite good. It is found that structure in the spectrum at wavelengths longer than 270 mμ is determined mainly by the quenching of excitons at the crystal surface, while below this wavelength the direct absorption of incident light by anthraquinone is important in determining spectrum structure.

Blue fluorescence in anthracene has also been excited by the 6943-A ruby laser line (111). Both the ordinary fluorescence and the delayed fluorescence are observed, the ordinary component arising from biphotonic absorption of the laser radiation. The delayed component arises from both biphotonic excitation of the singlet state followed by radiationless transition to the triplet (fourth-power dependence on laser intensity) and direct excitation of the triplet state (fluorescent intensity varying as the square of the incident intensity). The delayed fluorescence then follows as the result of bimolecular annihilation of the triplet excitons.

X. REFERENCES

(1) Agranovich, V. M., and Konobeev, I. V., *Opt. i Spektroskopiya*, **6**, 242 (1959).
(2) Agranovich, V. M., and Konobeev, I. V., *Opt. i Spektroskopiya*, **6**, 648 (1959).
(3) Agranovich, V. M., and Konobeev, I. V., *Opt. i Spektroskopiya*, **11**, 369, 504 (1961).
(4) Alexander, P. W., Lacey, A. R., and Lyons, L. E., *J. Chem. Phys.*, **34**, 2200 (1961).
(5) Anex, B. G., *Mol. Crystals*, **1**, 1 (1966).
(6) Avakian, P., and Merrifield, R. E., *Phys. Rev. Letters*, **13**, 541 (1964).
(7) Avery, D. G., *Proc. Phys. Soc.* (London), **B65**, 425 (1952).
(8) Birks, J. B., "The Theory and Practice of Scintillation Counting," Pergamon Press, Ltd., Oxford, 1964, p 214.
(9) Birks, J. B., *Proc. Phys. Soc.* (London), **79**, 494 (1962).
(10) Birks, J. B., King, T. A., and Munro, I. H., *Proc. Phys. Soc.* (London), **80**, 353 (1962).
(11) Birks, J. B., and Wright, G. T., *Proc. Phys. Soc.* (London), **B67**, 657 (1954).
(12) Black, F. A., *Phil. Mag.*, **44**, 263 (1953).
(13) Bode, H. W., "Network Analysis," D. Van Nostrand Co., Inc., New York, N. Y., 1945, p 303.
(14) Borisov, M. D., *Tr. Inst. Fiz. Akad. Nauk Ukr. SSR*, 102 (1953).
(15) Born, M., and Wolf, E., "Principles of Optics," Pergamon Press, Ltd., Oxford, 1964, p 36.
(16) Bowen, E. J., "Chemical Aspects of Light," Oxford University Press, Oxford, 1946, p 162.
(17) Bowlden, H. J., and Wilmshurst, J. K., *J. Opt. Soc. Am.*, **53**, 1073 (1963).
(18) Bree, A., Ph.D. Thesis, University of Sydney, 1958.
(19) Bree, A., and Lyons, L. E., *J. Chem. Soc.*, 2662 (1956).
(20) Brodin, M. S., and Dovgii, Y. O., *Opt. i Spektroskopiya*, **11**, 742 (1961).
(21) Brodin, M. S., and Lubchenko, A. F., *Opt. i Spektroskopiya*, **7**, 83 (1959).
(22) Brodin, M. S., and Marisova, S. V., *Opt. i Spektroskopiya*, **10**, 473 (1961).
(23) Brodin, M. S., and Prikhotjko, A. F., *Opt. i Spektroskopiya*, **2**, 448 (1957).
(24) Brodin, M. S., and Prikhotjko, A. F., *Opt. i Spektroskopiya*, **7**, 132 (1959).
(25) Brodin, M. S., Prikhotjko, A. F., and Soskin, M. S., *Opt. i Spektroskopiya*, **6**, 28 (1959).
(26) Broude, V. L., Pakhomova, O. S., and Prikhotjko, A. F., *Opt. i Spektroskopiya*, **2**, 323 (1957).
(27) Carswell, D. J., *J. Chem. Phys.*, **21**, 1890 (1953).
(28) Carswell, D. J., and Lyons, L. E., *J. Chem. Soc.*, 1734 (1955).
(29) Chapman, J. H., Forster, T., Kortum, G., Lippert, E., Melhuish, W. H., Nebia, G., and Parker, C. A., *Z. Anal. Chem.*, **197**, 431 (1963).
(30) Choi, S., and Rice, S. A., *Phys. Rev. Letters*, **8**, 410 (1962).
(31) Choi, S., and Rice, S. A., *J. Chem. Phys.*, **38**, 366 (1963).
(32) Compton, D. M. J., Schneider, W. G., and Waddington, T. C., *J. Chem. Phys.*, **27**, 160 (1957).
(33) Coulson, C. A., *Proc. Phys. Soc.* (London), **60**, 257 (1948).
(34) Coulson, C. A., "Valence," Oxford University Press, Oxford, 1952, p 233.
(35) Coulson, C. A., *Bull. Photoelectric Spectry. Group*, **13**, 358 (1961).
(36) Craig, D. P., *J. Chem. Soc.*, 2302 (1955).
(37) Craig, D. P., and Hobbins, P. C., *J. Chem. Soc.*, 539 (1955).
(38) Craig, D. P., and Hobbins, P. C., *J. Chem. Soc.*, 2309 (1955).
(39) Craig, D. P., and Walmsley, S., "Physics and Chemistry of the Organic Solid State," Vol. I, M. Labes, D. Fox, and A. Weissberger, Ed., John Wiley and Sons, Inc., New York, N. Y., 1963, p 585.
(40) Davydov, A. S., *Zh. Eksperim. i Teor. Fiz.*, **18**, 210 (1948).
(41) Davydov, A. S., "Theory of Molecular Excitons," McGraw-Hill Book Co., Inc., New York, N. Y., 1962, p 110.

(42) Dewar, M. J. S., and Longuet-Higgins, H. C., *Proc. Phys. Soc.* (London), **A67**, 795 (1954).
(43) Eitchiss, A., *Zh. Eksperim. i Teor. Fiz.*, **20**, 471 (1950).
(44) Ellis, C., and Wells, A., "The Chemical Action of Ultraviolet Rays," Reinhold Publishing Corp., New York, N. Y., 1941, p 504.
(45) Eremenko, V. V., and Medvedev, V. S., *Soviet Phys. Solid State*, **2**, 1426 (1961).
(46) Ferguson, J., and Schneider, W. G., *J. Chem. Phys.*, **28**, 761 (1958).
(47) Frenkel, J., *Phys. Rev.*, **37**, 17, 1276 (1931).
(48) Frenkel, J., *J. Phys. Chem.* (USSR), **9**, 158 (1936).
(49) Ganguly, S. C., and Chaudhury, N. K., *Rev. Mod. Phys.*, **31**, 990 (1959).
(50) Ham, N. S., and Ruedenberg, K., *J. Chem. Phys.*, **25**, 1 (1956).
(51) Hasegawa, K., and Schneider, W. G., *J. Chem. Phys.*, **40**, 2533 (1964).
(52) Hochstrasser, R. M., *Rev. Mod. Phys.*, **34**, 531 (1962).
(53) Hochstrasser, R. M., "Molecular Aspects of Symmetry," W. A. Benjamin, Inc., New York, N. Y., 1966, p 296.
(54) Hopfield, J. J., and Thomas, D. G., *Phys. Rev.*, **132**, 563 (1963).
(55) Jones, L. C., and Taylor, L. W., *Anal. Chem.*, **27**, 228 (1958).
(56) Jones, R. N., *Chem. Rev.*, **41**, 353 (1947).
(57) Kearns, D. R., *J. Chem. Phys.*, **39**, 2697 (1963).
(58) Kepler, R. G., *Phys. Rev.*, **119**, 226 (1960).
(59) Kepler, R. G., *IEEE Trans., Nucl. Sci.*, **11** (5), 1 (1964).
(60) Kepler, R. G., and Merrifield, R. E., *J. Chem. Phys.*, **40**, 1173 (1964).
(61) Kepler, R. G., and Switendick, A. C., *Phys. Rev. Letters*, **15**, 56 (1965).
(62) Kharitonova, O. P., *Opt. i Spektroskopiya*, **5**, 29 (1958).
(63) Kilin, S. F., and Rozman, I. M., *Opt. i Spektroskopiya*, **6**, 40 (1959).
(64) Klevens, H. B., and Platt, J. R., *J. Chem. Phys.*, **17**, 470 (1949).
(65) Knox, R. S., *Solid State Phys.*, Suppl. 5 (1963).
(66) Kommandeur, J., and Schneider, W. G., *J. Chem. Phys.*, **28**, 582 (1958).
(67) Kommandeur, J., and Schneider, W. G., *J. Chem. Phys.*, **28**, 590 (1958).
(68) Levine, M., Jortner, J., and Szoke, A., *J. Chem. Phys.*, **45**, 1591 (1966).
(69) Lipsett, F. R., Compton, D. M. J., and Waddington, T. C., *J. Chem. Phys.*, **26**, 1444 (1957).
(70) Longuet-Higgins, H. C., *Proc. Roy. Soc.* (London), **60**, 270 (1948).
(71) Lower, S. K., and El-Sayed, M. A., *Chem. Rev.*, **66**, 199 (1966).
(72) Lyons, L. E., *J. Chem. Phys.*, **23**, 220 (1955).
(73) Lyons, L. E., and Morris, G. C., *J. Chem. Soc.*, 3648 (1957).
(74) Lyons, L. E., and Morris, G. C., *J. Chem. Soc.*, 5001 (1957).
(75) Lyons, L. E., and Morris, G. C., *J. Chem. Soc.*, 1551 (1959).
(76) Marcus, A., and Heller, W. R., *Phys. Rev.*, **84**, 809 (1951).
(77) McClure, D. S., *J. Chem. Phys.*, **22**, 1256 (1954).
(78) McClure, D. S., *Solid State Phys.*, **8**, 1 (1959).
(79) Mathieson, A. M., Robertson, J. M., and Sinclair, V. C., *Acta Cryst.*, **3**, 245 (1950).
(80) Melhuish, W. H., *J. Chem. Phys.*, **40**, 1369 (1964).
(81) Moffit, W., *J. Chem. Phys.*, **22**, 320 (1954).
(82) Moss, T. S., "Optical Properties of Semi-Conductors," Butterworth & Co., Ltd., London, 1961, p 22.
(83) Mott, N. F., *Trans. Faraday Soc.*, **34**, 500 (1938).
(84) Mulliken, R. S., *Phys. Rev.*, **43**, 279 (1933).
(85) Nakada, I., *J. Phys. Soc. Japan*, **17**, 113 (1962).
(86) Northrop, D. C., and Simpson, O., *Proc. Phys. Soc.* (London), **B68**, 974 (1955).
(87) Northrop, D. C., and Simpson, O., *Proc. Roy. Soc.* (London), **234**, 136 (1956).
(88) Northrop, D. C., and Simpson, O., *Proc. Roy. Soc.* (London), **244**, 377 (1958).
(89) Obreimov, I. W., Prikhotjko, A. F., and Rodnikova, I. W., *Zh. Eksperim. i Teor. Fiz.*, **18**, 409 (1948).
(90) Pariser, R., *J. Chem. Phys.*, **24**, 250 (1956).
(91) Parker, C. A., *Advan. Photochem.*, **2**, 302 (1964).
(92) Parker, C. A., and Rees, W. T., *Analyst*, **85**, 587 (1960).
(93) Peacock, T. E., and Wilkinson, P. T., *Proc. Phys. Soc.* (London), **83**, 525 (1964).
(94) Peierls, R., *Ann. Phys.*, **13**, 905 (1932).
(95) Peticolas, W. L., Goldsborough, J. P., and Rieckhoff, K. E., *Phys. Rev. Letters*, **10**, 43 (1963).
(96) Platt, J. R., *J. Chem. Phys.*, **17**, 484 (1949).
(97) Pope, M., "Luminescence of Organic and Inorganic Compounds," John Wiley and Sons, Inc., New York, N. Y., 1962, p 276.
(98) Pople, J. A., *Proc. Phys. Soc.* (London), **A68**, 81 (1955).
(99) Reucroft, P. J., *J. Chem. Phys.*, **36**, 1114 (1962).
(100) Robinson, T. S., *Proc. Phys. Soc.* (London), **B65**, 910 (1952).
(101) Robinson, T. S., and Price, W. C., *Proc. Phys. Soc.* (London), **B66**, 969 (1953).
(102) Schneider, W. G., *J. Chem. Phys.*, **25**, 358 (1956).
(103) Schulman, J. H., Etzel, H. W., and Allard, J. G., *J. Appl. Phys.*, **28**, 792 (1957).
(104) Sidman, J. W., *Phys. Rev.*, **102**, 96 (1956).
(105) Sidman, J. W., *J. Am. Chem. Soc.*, **78**, 4567 (1956).
(106) Sidman, J. W., *J. Chem. Phys.*, **27**, 820 (1957).
(107) Silver, M., Olness, D., Swicord, M., and Jarnagin, R. C., *Phys. Rev. Letters*, **10**, 12 (1963).
(108) Simon, I., *J. Opt. Soc. Am.*, **41**, 336 (1951).
(109) Simpson, O., *Proc. Roy. Soc.* (London), **238**, 402 (1957).
(110) Sinclair, V. C., Mathieson, A. M., and Robertson, J. M., *Acta Cryst.*, **3**, 251 (1950).
(111) Singh, S., Jones, W. J., Siebrand, W., Stoicheff, B. P., and Schneider, W. G., *J. Chem. Phys.*, **42**, 330 (1965).
(112) Steketee, J. W., and de Jonge, J., *Philips Res. Rept.*, **17**, 363 (1962).
(113) Stevens, B., and Hutton, E., *Mol. Phys.*, **3**, 71 (1960).
(114) Toll, J. S., *Phys. Rev.*, **104**, 1760 (1956).
(115) Tousey, R., *J. Opt. Soc. Am.*, **29**, 235 (1939).
(116) Wannier, G. H., *Phys. Rev.*, **52**, 191 (1937).
(117) Weber, G., and Teale, F., *Trans. Faraday Soc.*, **54**, 640 (1958).
(118) Wilkinson, F., *Advan. Photochem.*, **3**, 241 (1964).
(119) Williams, D. F., Adolph, J., and Schneider, W. G., *J. Chem. Phys.*, **45**, 575 (1966).
(120) Windsor, M. W., "Physics and Chemistry of the Organic Solid State," Vol. II, M. Labes, D. Fox, and A. Weissberger, Ed., John Wiley and Sons, Inc., New York, N. Y., 1965, p 343.
(121) Wolf, H. C., *Z. Naturforsch.*, **13a**, 414 (1958).
(122) Wolf, H. C., *Solid State Phys.*, **9**, 1 (1959).
(123) Wright, G. T., *Phys. Rev.*, **100**, 587 (1955).
(124) Wright, G. T., *Proc. Phys. Soc.* (London), **B68**, 241 (1955).
(125) Wright, G. T., *Proc. Phys. Soc.* (London), **B68**, 701 (1955).
(126) Wright, W. H., Ph.D. Thesis, Rhodes University, S. Africa, 1965.
(127) Wright, W. H., *J. Chem. Phys.*, **45**, 874 (1966).
(128) Wright, W. H., *J. Chem. Phys.*, **46**, 2951 (1967).
(129) Zinzer, H. J., *Z. Naturforsch.*, **11a**, 306 (1956).